



Identification of Rip Current Hazards Using Fluorescent Dye And Unmanned Aerial Vehicle (A Case Study Of Drini Beach, Gunungkidul, Indonesia)

5 ¹Hendy Fatchurohman¹, Alfiatun Nur Khasanah¹, Ahmad Cahyadi²

¹Department of Earth Science, Vocational College, Universitas Gadjah Mada. Sekip Utara Jalan Kaliurang, Bulaksumur, Yogyakarta, Indonesia, 55281

10 ²Department of Environmental Geography, Faculty of Geography, Universitas Gadjah Mada. Sekip Utara Jalan Kaliurang, Bulaksumur, Yogyakarta, Indonesia, 55281

Correspondence to: Hendy Fatchurohman (hendy.fatchurohman@ugm.ac.id)

Abstract. Coastal tourism is a leading sector substantially contributing to the regional income of Gunungkidul Regency, Indonesia. However, with more tourists visiting the beach, more lives are threatened by coastal hazards. Rip currents are a channel of powerful, narrow, fast-moving water that can carry floating objects away from the shore, presenting one of the most common coastal hazards to swimmers. Unfortunately, most tourists are unaware of rip currents and their threats and how to avoid them. This study was designed to identify the types and dimensions of rip current in one of the regency's tourist attractions, Drini Beach. For this purpose, an environmentally friendly fluorescent dye, Uranine, was injected from the shoreline, then the velocity and direction of its movements were observed from aerial video footage captured with a drone. Results showed stationary rip currents with a narrow channel, called a channel rip, with the mean dimensions: 250 m from the shoreline to the head and 10.25 m in width. A break in the reef flat can mostly generate rip currents at Drini Beach. It creates an area that is deeper than the surrounding reef flats through which water and the transported coastal sediments can flow easily offshore. Rip currents identified in this research provide the basis for disaster mitigation measures to reduce fatality

25 1 Introduction

Rip currents pose one of the biggest threats to coastal areas worldwide. They are the leading cause of many marine accidents on a sandy coast (Arozarena et al., 2015; Brighton et al., 2013; Li, 2016; Scott et al., 2011). Thousands of drowning cases have been reported in different countries, with tens to hundreds of beach tourists killed each year (Arun Kumar and Prasad, 2014; Cervantes et al., 2015; Fallon et al., 2018; Gallop et al., 2016; Da Silva, 2008; Winter et al., 2014). A rip current



30 can quickly pull even good swimmers offshore (Castelle et al., 2016b) because, when caught in one, they may panic and exhaust themselves by swimming against the current, resulting in drowning and even deaths. Lifeguards rescue some, but the ones drowned in beaches without lifeguards on duty cannot be saved (Castelle et al., 2018).

A rip current is a strong, narrow current that moves offshore and reportedly has ecological impacts (Leatherman, 2014; Winter et al., 2014). It generally starts from the shoreline and extends to the surf zone or further seaward because of various factors, such as bathymetric conditions, wave height, and coastal typology (Bruneau et al., 2014; Wang et al., 2018). Variations in the bottom topography near the coast produce breaking waves of different patterns and energies, creating a funnel for backflow against the sea (MacMahan et al., 2005). Depending on the forming factors, a rip current develops at different times and place (Pitman et al., 2016) and can persist with strong coastal morphological controls (Castelle et al., 2016b). It is analogous to a “river in the sea” because it has characteristic energy and velocity that differ from its surroundings (Bonetti, 2013). On average, it can flow at about 0.5 m/s to 2 m/s (Leatherman, 2017). Further, a rip current plays a significant role in the mass exchange of water, sediments, and pollutants between land and ocean (Sabet and Barani, 2011).

Gunungkidul Regency has the longest coastline in the Special Region of Yogyakarta, Indonesia, i.e., 87.12 km (Marfai et al., 2020). Located in southern Java Island, this coastal region is exposed to multiple hazards. The subduction zone in the south makes some locations susceptible to various destructive tectonic and volcanic activities (Marfai et al., 2008). Tsunamis are among the biggest threats to the island’s south coast (Marfai et al., 2019b), but based on the number of cases, marine accidents occur more frequently. In Gunungkidul, marine accidents have been recorded to cause fatalities every year. Seventy-seven marine accidents with four deaths were reported in 2017, which increased dramatically to 128 incidents with three fatalities and one missing (Widiyanto, 2020). Although the accidents reduced to 90 in 2019, casualties multiplied to 15 deaths. Then, in 2020, they fell to 53 cases, with 74 injured and seven deaths. However, the main factor of such decline is believed to be the decreased number of beach tourists during the COVID-19 pandemic (Aprita, 2020a). In-depth studies of physical characteristics and vulnerabilities are necessary in order to provide accurate information in dealing with rip currents. Scholars have analyzed rip currents in Parangtritis, a coastal area in the Special Region of Yogyakarta, by utilizing satellite images and a series of aerial photos taken with kites (Retnowati et al., 2013; Widartono et al., 2019). However, no research has focused explicitly on the rip currents in Gunungkidul to date, indicating the need for a similar study in the regency.

Several studies on rip current disasters in various countries have begun to utilize remote sensing data and UAV technology. Both means provide many conveniences and more detailed information (Kasvi et al., 2019; Leatherman, 2017; Pitman et al., 2016). However, the data used to analyze rip currents as a coastal hazard are minimal, especially the most current parameter values and characteristics with high spatial resolution. Data that are remotely sensed by an unmanned aerial vehicle (UAV) are proposed to address this problem. UAVs capture real-time information at a relatively low cost to produce high-resolution aerial photos and even elevation data with sharp detail (e.g., digital elevation model/DEM) (Chen et al., 2018; Gomez and Purdie, 2016; Kršák et al., 2016). High-resolution UAV-derived data prove suitable for disaster studies in coastal areas (Marfai et al., 2018, 2019a).



A rip current is mostly invisible on the water surface, making it difficult for tourists to observe and spot while on the beach (Barlas and Beji, 2016; Brannstrom et al., 2015). Most beach tourists are aware of this current but cannot straightforwardly identify it from photos of different types of water current (Brighton et al., 2013; Caldwell et al., 2013). Fluorescent dyes have been used to identify and delineate rip currents in many parts of the world (Bonetti, 2013; Kumar et al., 2021; Leatherman, 2017). Dye solutions produce striking visual effects that can effectively trace the direction and velocity of a rip current and, at the same time, attract the attention of tourists and the media (Brander et al., 2014). This process seems to clearly show a danger that is otherwise invisible to the naked eye.

This study was intended to identify the rip currents along the coast of Drini Beach, Gunungkidul, using a fluorescent dye and a UAV. The observed features include type, dimension, and location of appearance. An accurate description is expected to help formulate necessary mitigation and create the basis for coastal disaster risk reduction measures. Besides, the data collected throughout this study can help swimmers and beach tourists, in general, to be aware of and alert to the appearances of rip currents and their hazardous nature.

2 Methods

2.1. Study Area

Increased tourism activities in Gunungkidul Regency (Special Region of Yogyakarta, Indonesia) multiply the number of people exposed to the danger of rip currents. This study focuses on the coastal area at Drini Beach, in which dry farming and agroforestry practices are abundant. Drini Beach is located approximately 60 km southeast of the special region's capital and is part of the Gunungsewu Karst Area that entirely lies in the carbonate rocks of the Wonosari Formation (Tmwl). There are two main lithofacies: coral reefs and bioclastic limestones that constitute most of the formation, wherein limestone stratification leans to the south. The karst area is also divided by a northwest-southeast fault with a northeastern synclinal axis in the middle (Kusumayudha et al., 2000).

Figure 1 shows that the Drini coastal area develops in labyrinth-cone with rectangular, oval, and straight ridge patterns controlled by major faults and joints. Residual hills in this landform generally have steeper slopes than other landforms in the Gunungsewu Karst Area. The major faults and joints controlling the conical labyrinth development are associated with the subduction zone south of the karst area. Maximum compression and stress from this tectonic activity led to intense rock displacements, i.e., faults and joints (Haryono and Day, 2004). The strong control over the labyrinth-cone karst creates a characteristic landscape: reef flats, ridges, and karst hills dominate most of the Gunungkidul coastal area. With these characteristics, the beaches are small bays with narrow and steep stretches (Marfai et al., 2020). Coastal typology on a sandy beach with corals in the tropics and subtropics likely forms nearshore currents, a precondition of rip currents during low tides (Leon et al., 2008).



2.2 Rip Current Identification

The identification of the rip currents started by injecting fluorescent dye solution, which is Uranine ($C_{20}H_{12}O_5$).
 95 Fluorescent dye is an organic tracer dye widely used in hydrogeological studies, especially groundwater tracing in a karst
 drainage system. It is composed of highly soluble salt and can emit light (fluoresce) in water. In addition to being visible to
 the naked eye, this tracer dye can also be detected at very low concentrations (Thi et al., 2006). It is widely circulated in the
 market and is available for commercial purposes. Besides, it is safe, conservative, easy to detect, inexpensive, and easy to use
 (Ford and Williams, 2007). Uranine has a very low limit of detection in ideal conditions, i.e., up to 0.001 g/L. It has a bright
 100 green color when dissolved in water at concentrations above 10µg/L and red at higher than 1 g/L. Uranine is highly soluble
 and harmless to humans and the environment. For the rip current tracing, the amount of uranine injected at the shoreline was
 calculated using Eq. 1 (Goldscheider and Drew, 2007).

$$M = L \times k \times B \quad (1)$$

105 where M is the required mass (in kg), L is the distance to be detected (in km), k is the coefficient for the tracer dye used, and
 B is the hydrological condition factor.

Upon injection, the tracer solution was carried offshore by a rip current; then, its flow was monitored from aerial
 photos and videos taken with a UAV/drone. Videos are especially helpful in identifying the direction of the current. The drone
 was a multirotor equipped with a hover mode, namely the DJI Mavic Pro Enterprise, and was controlled with the DJI-GO 4
 110 app to stay on course at an altitude of 250 m to record the video of the entire study area.

2.3. Aerial Photo Acquisition

In addition to video footage, the drone was set to automatically take aerial photos using auto-pilot control in the Drone
 Deploy software to produce orthophotos. The software can automatically create a flight path according to the predefined area
 of interest. At Drini Beach, the aerial photos were acquired at an altitude of 250 m, with an average flight velocity of 15 m/s
 115 and 75% frontal overlap and 65% side overlap.

During the photo acquisition, the terrestrial coordinates of Ground Control Points (GCPs) were detected with a
 geodetic GPS to produce accurate location data. Marked targets or markers were distributed evenly throughout the area of
 interest, and the coordinates of their locations were read using a geodetic GPS and made as GCPs. The placement of markers
 must consider horizontal and vertical distribution to obtain maximum accuracy. Figure 2 shows examples of markers and a
 120 GCP measurement.

To determine the rip current's width and length, the distance in the field was measured following the photogrammetry
 concept: in an aerial upright photo, terrestrial distance depends on the altitude at which the drone flies and the focal length of
 the camera used. The ground sample distance was determined using Eq. 2.

$$S = f/Hg \quad (2)$$



125 where S is the ground spatial distance or the smallest pixel size produced, f is the focal length of the camera, and H_g is the height of the drone flight.

3 Results

3.1 Orthomosaic Image

130 The Flight Mission at Drini Beach was made following a north-south direction with a flight azimuth of 103° or perpendicular to the coast. It is imperative that the flight direction be determined prior to take off for effective lighting missions. Flight direction affects headwinds and tailwinds hitting the vehicle and the speed of the vehicle in completing the mission (Clark, 2017). In this flight mission, the vehicle was adjusted to reach a maximum speed of 15 m/s. The area of interest covers 100 hectares, which were covered in 315 photos taken for about 21 minutes. Five markers were made with a clear pattern for easy identification from the aerial photos and placed at every corner and in the middle of the area of interest. The coordinates
 135 were determined using the Real-Time Kinematic method. The Ground Control Point measurement and the flight route are depicted in Fig. 2 .

Upon data acquisition, all aerial photos were processed in Agisoft Metashape to produce an orthophoto. Because the aerial photos were captured using DJI Mavic 2 Pro at an altitude of 250 m with a lens focal length of 4.5 mm, the orthophoto produced has a ground sampling distance (GSD) of 7 cm. This figure indicates raster data with very high spatial resolution
 140 suitable for topographic measurements and identification of short-term changes in coastal areas (Chen et al., 2018).

The orthorectification process generates dense point clouds as elevation points and finally creates the entire DEM (Turner et al., 2016). The generated DEM is a Digital Surface Model (DSM) in which the elevation is measured from the surface of the land cover captured by the visible camera sensor. In this research, the DSM derived from the aerial photos has a 35-cm spatial resolution. Figure 3 shows the generated orthophoto and DSM in Agisoft. First, the orthophoto was
 145 georeferenced with five GCPs spread evenly in the area of interest. Second, it was used to validate the measured dimensions of the rip current identified using a fluorescent tracer dye. Also, the videos recording the flow of the dye solution have a central projection, allowing errors to potentially occur at locations far from the camera's nadir (Aber et al., 2019).

3.2. Rip Current Tracing

150 The rip current was traced using the fluorescent dye uranine, which has a coefficient value (k) of 1. An open body of water has a hydrological condition factor (B) in the range of 0.1–0.9, and the highest B value (0.9) was selected to produce a dense color (maximum concentration of uranine) for easy identification. The rip current was estimated to be 0.4 km or 400 m in length (from the shoreline). Therefore, based on the calculation results using Eq. 1, the required mass of uranine was 360 grams.

155 The tracer dye solution was injected on July 24, 2020, at about 12:17 am during the tidal transition. This time was selected considering that the rip current velocity is the most dangerous and claims the most victims during the transition from



medium to low tide (Scott et al., 2009). To determine the optimum conditions for the dye injection, tide prediction was obtained from the Geospatial Information Agency (<http://tides.big.go.id/>). The research location has semidiurnal tides, where the peak high tides occur at around 10:00 am and 11:30 pm, while the peak low tides at 4:20 am and 5:00 pm. The station at Sadeng (25 km) was the closest to the study area; hence, selected as an observation station.

160 The tracer dye solution was injected to the water by sudden injection to obtain the optimum concentration and color, making it easy to detect. It was injected east of the gap in the surf zone commonly used by fishing boats to enter the sea. Shortly before the injection, the drone took off and started recording videos from an altitude of 250 m. Soon after, the green solution appeared in the video footage and moved diagonally to the west then further towards the sea. This movement follows the seaward margin of the reef flat. The dye solution was continuously injected until all 360 g of the prepared uranine was in
 165 the water. Figure 4 reveals that the observed rip current immediately formed clear structures: developing from feeder currents to rip neck then rip head.

4. Discussion

Monitoring from above revealed that the rip current was approximately 250 m long, measured from the shoreline to the rip head, and 10.25m wide. The tracer dye solution carried by the rip current formed a long, narrow channel—a
 170 characteristic of the rip neck, which slightly bent westward and extended more than 250 m offshore. The rip current velocity was estimated from the orthophoto and the video. First, after comparing the distances between the objects on the orthophoto, the velocity was calculated, and the results showed fluctuating speeds from the injection until the dye reached the rip neck. Second, observation on the sequence of the video footage revealed that the rip current fully formed (feeder currents-the neck-the head) in approximately eight minutes before returning to the shore through the surf zone. The video sequence was first
 175 calibrated with the orthophoto data, and the tip of the injected dye (green color) was tracked to estimate the rip current velocity. Figure 5 depicts that the rip current was the most rapid when passing through the neck in the surf zone, i.e., 0.42 m/s to 0.66 m/s. Bigger force and narrower circulation in the neck are believed to be responsible for the fast velocity (Kennedy et al., 2008; MacMahan et al., 2006). In the rip neck, the current can be as fast as 2 m/s, creating the deadliest area for swimmers caught in the rip current (Gensini and Ashley, 2010).

180 From 0 to 4 minutes after injecting the tracer dye solution, the current velocity was only 0.11 m/sec. However, it increased dramatically to 0.42 m/s when excess feeder currents flowed seaward at a perpendicular angle and entered the neck. Table 1 shows the maximum current velocity recorded was 0.66 m/sec in Minute 9 or when it entered the neck. Based on several observations, it has been confirmed that water indeed flows the most rapidly in the neck zone (Chen et al., 1999; Kumar et al., 2021).

185 In order to determine the rip current velocity more accurately, it is necessary to carry out detailed measurements using different methods. Tens to hundreds of experiments on different wave conditions prove adequate to obtain the exact measurements (Dudkowska et al., 2020). An example includes repeatedly releasing drifters with an attached or built-in GPS



device to the sea to determine the current velocity and direction (Castelle et al., 2016a; Gallop et al., 2018; Kennedy and Thomas, 2004).

190 This study aims to identify the rip currents at Drini Beach and the factors influencing their formation. On the surface, a rip current often appears foamy in the surf zone. From the aerial image, the area without breakers indicates a deeper zone that possibly forms rip current (Retnowati et al., 2013). Based on the temporal analysis of Google Earth satellite imagery depicted in Fig. 6., the rip current at Drini Beach is persistent or stationary. Bathymetric conditions that are stable or less likely to change are known to control its formation. For this reason, the rip current is categorized into channel rips (Castelle et al., 195 2016b). Most channel rips are associated with sand substrates in the bottom between the coral reef flats. This type of rip current is commonly referred to as a reef rip current (Leon et al., 2008), which is persistent and stationary.

Reef flats strongly determine the formation of rip currents. There are insufficient feeder currents at the peak low tide to form a rip current because the seawater is below the reef flat surface and fills deeper breaks in the reef flat. In this context, the breaks regulate the mass exchange of water in reef flats, especially during low tides (Leon et al., 2008). Reef rip currents 200 can appear and disappear depending on the heights of the tides (Castelle et al., 2016b). Figure 7 shows the effect of tides on the formation of rip currents at Drini Beach.

Figure 8 shows during the peak of low tides, beach tourists usually swim in the gap of the reef flat where the rip current usually appears because it is the only part near the shore that is submerged, unlike the reef flat. However, despite the low feeder currents, this condition remains a threat to swimmers because rip currents tend to form when the water begins to 205 ebb. Therefore, tourists and lifeguards need to make sure that the area used for swimming is safe and is at the peak low tide. Records obtained from the tide observation station at Sadeng port (25 km east of Drini Beach) showed that the peak high tide is averagely 240 cm, while the peak low tide is 70 cm (<http://tides.big.go.id/>, 2021).

The channel rip currents at Drini Beach are persistent and stationary and can be predicted through tide observations. This information helps to formulate mitigation measures to increase tourist safety. So far, no boards or signs are warning the 210 tourists of rip currents and their dangers. Strategies to promote tourist safety need to be structured comprehensively, including education to beach tourists, risk assessment and monitoring, signs of dangerous areas at the beach area or segments where rip currents usually appear, and management and emergency response (Li, 2016). For a start, colored flags can be used to signal threats. Each color can represent different levels of threat, e.g., poles with a blue flag are installed in safe areas, while the ones with a red flag indicate areas where swimming is prohibited (Castelle et al., 2019). This flagpole is flexible and convenient in 215 that it can be moved according to the tide conditions. When it is safe for swimming, locations with previously red flags can be replaced with blue flags at certain times. However, it is only allowed after the coast guards have sufficiently observed the tide behavior and confirmed that said locations are safe.

In addition to drawing tourists' attention, the in-situ measurements have attracted public attention on various social media platforms. The process of tracer dye injection on the shore and a brief explanation about rip currents in an online news 220 channel on Instagram have been viewed more than 66 thousand times (Disini, 2020). Various online newspapers also reported the rip current tracing process, which attracted thousands of readers (Ajeng and Dharmawangsa, 2020; Aprita, 2020b; Aryono,



2020; Azizah, 2020; Kandar, 2020; Pertana, 2020; Yuwono, 2020). Injecting fluorescent dye in the process indeed creates a dramatic effect and directly shows rip current hazards to the public. Such “wow effect” proves effective for providing education and even disseminating experiment findings to broader communities (Brander et al., 2014).

225 5. Conclusion

This study is a preliminary study to identify rip current hazards alongside the coastal area of Gunungkidul. Understanding the rip current nature such as type, dimension and velocity is necessary to minimize fatalities. Rip currents pose dangers to The coastal area of Gunungkidul, as evident from the increasing number of tourists and records of those affected by marine accidents. This study was conducted at Drini Beach, Gunungkidul Regency, Yogyakarta Special Province, Indonesia. Based on the current tracing, the beach has a channel rip, which is persistent stationary and is controlled by the bathymetric conditions. It develops in the break in the reef flats with sand substrates in its bottom and in the break that is deeper than the surrounding reef flats. Tides are also a known factor in its formation. The photogrammetric measurements show the fluorescent dye movements and dimensions. The rip current is 250m long, with an average width of 10.25 m. It can flow with an average speed of 0.31 m/s. As soon as the tracer entering the neck zone, the velocity rapidly increased from 0.18 m/s to 0.42 m/s. The maximum velocity of the rip current was recorded when passing through the neck, i.e., 0.66 m/s. Bigger force and narrower circulation in the neck are believed to be responsible for the fast velocity. Controlled by bathymetric conditions, the rip current at Drini Beach formed in the gap between reef flats. Therefore, the rip current is persistent in the same place and appear only when the wave meets some particular condition. The persistent or stationary nature of the rip current makes it easier for the coast guard to manage concomitant risks. Flags can be used to warn tourists of swimming restrictions in the reef flat gaps and can be moved according to tide conditions. This research has identified the location and type of the rip current at Drini Beach. Further studies are required in order to determine the character, velocity, and time variations in the rip current formation. Fluorescent dye proves effective for tracing rip current’s movement because it produces a clear visible effect. It also gives beach tourists evidence or an accurate picture of an invisible hazard. This experiment also managed to attract tens of thousands of people on social media platforms, promoting safety and education campaigns to the community.

245 Author contribution:

Hendy Fatchurohman carried out the research design in general and was in charge of coordinating the field survey. Alfiatun Nur Khasanah participated in the field data collection and carried out the production of the maps. Ahmad Cahyadi participated in the field data collection and was responsible for the preparation of the manuscript. All authors read and approved the final manuscript.



250 Acknowledgement

This research is part of the 2021 Competitive Research Grant of Vocational College, Universitas Gadjah Mada (Hibah Penelitian Kompetitif Sekolah Vokasi, Universitas Gadjah Mada Tahun 2021) contract number: 67/UN1.SV/KPT/2021 83/UN1.SV/KPT/2020, titled "Pemanfaatan Teknologi Pesawat Tanpa Awak untuk Pemetaan Bahaya Arus Retas (rip current) di Pantai Pulang Sawal, Gunungkidul, D.I. Yogyakarta". The authors gratefully acknowledge the research funding and support
255 from the Vocational College, Universitas Gadjah Mada. We also thank all the students from the Department of Earth Science, Vocational College, Universitas Gadjah Mada that participated in data collection, data processing, and all the paperwork related to this research. This work was also supported by the rescue team of Baron Beach and the surrounding area (SATLINMAS BARON). We thank them for their companion and help during the data collection. Last but not least, we appreciate all the media that reported our study to their page and social media to reach the main goal of this research, which is
260 to bring awareness to the public regarding the rip current hazard.

References

- Aber, J. S., Marzloff, I., Ries, J. B. and Aber, S. E. W.: Small-Format Aerial Photography and UAS Imagery, Second Edi., Elsevier, Cambridge., 2019.
- Ajeng, B. and Dharmawangsa, J.: Waspada Fenomena Arus Retas di Pantai Selatan – Clapeyron, [online] Available from:
265 <http://www.clapeyronmedia.com/waspada-fenomena-arus-retas-di-pantai-selatan/> (Accessed 23 June 2021), 2020.
- Aprita, A.: Laka Laut di Pantai Gunungkidul Turun Selama 2020, SAR Tetap Ketat Awasi Pengunjung, [online] Available from: <https://jogja.tribunnews.com/2021/01/26/laka-laut-di-pantai-gunungkidul-turun-selama-2020-sar-tetap-awasi-ketat-pengunjung> (Accessed 15 June 2021a), 2020.
- Aprita, A.: Makan Ratusan Korban, Pemetaan Wilayah Rip Current Laut Selatan Penting Dilakukan - Halaman all - Tribun
270 Jogja, [online] Available from: <https://jogja.tribunnews.com/2020/07/27/makan-ratusan-korban-pemetaan-wilayah-rip-current-laut-selatan-penting-dilakukan?page=all> (Accessed 23 June 2021b), 2020.
- Arozarena, I., Houser, C., Echeverria, A. G. and Brannstrom, C.: The rip current hazard in Costa Rica, Nat. Hazards, 77(2), 753–768, doi:10.1007/s11069-015-1626-9, 2015.
- Arun Kumar, S. V. V. and Prasad, K. V. S. R.: Rip current-related fatalities in India: A new predictive risk scale for forecasting
275 rip currents, Nat. Hazards, 70(1), 313–335, doi:10.1007/s11069-013-0812-x, 2014.
- Aryono, S.: Uji Coba Ahli UGM, Ombak Pantai Ini Mampu Menyeret Perenang Profesional, [online] Available from: <https://koranbernas.id/uji-coba-ahli-ugm-ombak-pantai-ini-mampu-menyeret-perenang-profesional> (Accessed 23 June 2021), 2020.
- Azizah, U. N.: Jadi Penyebab Laka Laut, Tim Peneliti Petakan Rip Current di Pantai Selatan Gunungkidul - pidjar.com,
280 [online] Available from: https://pidjar.com/jadi-penyebab-laka-laut-tim-peneliti-petakan-rip-current-di-pantai-selatan-gunungkidul/27098/?fbclid=IwAR0F8ON-PM3_t_uP3N5vs_jVzA3gyuf8LUL0Rj5qgV7OP8lecRndE1atgJY (Accessed 23



- June 2021), 2020.
- Barlas, B. and Beji, S.: Rip current fatalities on the Black Sea beaches of Istanbul and effects of cultural aspects in shaping the incidents, *Nat. Hazards*, 80(2), 811–821, doi:10.1007/s11069-015-1998-x, 2016.
- 285 Bonetti, J.: Spatial and Numerical Methodologies on Coastal, , (September 2017), 117–149, doi:10.1007/978-94-007-5234-4, 2013.
- Brander, R. W., Drozdowski, D. and Dominey-Howes, D.: “Dye in the Water”: A Visual Approach to Communicating the Rip Current Hazard, *Sci. Commun.*, 36(6), 802–810, doi:10.1177/1075547014543026, 2014.
- Brannstrom, C., Lee Brown, H., Houser, C., Trimble, S. and Santos, A.: “You can’t see them from sitting here”: Evaluating
 290 beach user understanding of a rip current warning sign, *Appl. Geogr.*, 56, 61–70, doi:10.1016/j.apgeog.2014.10.011, 2015.
- Brighton, B., Sherker, S., Brander, R., Thompson, M. and Bradstreet, A.: Rip current related drowning deaths and rescues in Australia 2004–2011, *Nat. Hazards Earth Syst. Sci.*, 13(4), 1069–1075, doi:10.5194/nhess-13-1069-2013, 2013.
- Bruneau, N., Bertin, X., Castelle, B. and Bonneton, P.: Tide-induced flow signature in rip currents on a meso-macrotidal beach, *Ocean Model.*, 74, 53–59, doi:10.1016/j.ocemod.2013.12.002, 2014.
- 295 Caldwell, N., Houser, C. and Meyer-Arendt, K.: Ability of beach users to identify rip currents at Pensacola Beach, Florida, *Nat. Hazards*, 68(2), 1041–1056, doi:10.1007/s11069-013-0673-3, 2013.
- Castelle, B., McCarroll, R. J., Brander, R. W., Scott, T. and Dubarbier, B.: Modelling the alongshore variability of optimum rip current escape strategies on a multiple rip-channelled beach, *Nat. Hazards*, 81(1), 663–686, doi:10.1007/s11069-015-2101-3, 2016a.
- 300 Castelle, B., Scott, T., Brander, R. W. and McCarroll, R. J.: Rip current types, circulation and hazard, *Earth-Science Rev.*, 163, 1–21, doi:10.1016/j.earscirev.2016.09.008, 2016b.
- Castelle, B., Brander, R., Tellier, E., Simonnet, B., Scott, T., McCarroll, J., Campagne, J. M., Cavailhes, T. and Lechevrel, P.: Surf zone hazards and injuries on beaches in SW France, *Nat. Hazards*, 93(3), 1317–1335, doi:10.1007/s11069-018-3354-4, 2018.
- 305 Castelle, B., Scott, T., Brander, R., McCarroll, J., Robinet, A., Tellier, E., De Korte, E., Simonnet, B. and Salmi, L. R.: Environmental controls on surf zone injuries on high-energy beaches, *Nat. Hazards Earth Syst. Sci.*, 19(10), 2183–2205, doi:10.5194/nhess-19-2183-2019, 2019.
- Cervantes, O., Verduzco-Zapata, G., Botero, C., Olivios-Ortiz, A., Chávez-Comparan, J. C. and Galicia-Pérez, M.: Determination of risk to users by the spatial and temporal variation of rip currents on the beach of Santiago Bay, Manzanillo, Mexico: Beach hazards and safety strategy as tool for coastal zone management, *Ocean Coast. Manag.*, 118, 205–214, doi:10.1016/j.ocecoaman.2015.07.009, 2015.
- 310 Chen, B., Yang, Y., Wen, H., Ruan, H., Zhou, Z., Luo, K. and Zhong, F.: High-resolution monitoring of - Beach topography and its change using unmanned aerial vehicle imagery, *Ocean Coast. Manag.*, 160(December 2017), 103–116, doi:10.1016/j.ocecoaman.2018.04.007, 2018.
- 315 Chen, Q., Dalrymple, R. A., Kirby, J. T., Kennedy, A. B. and Haller, M. C.: Boussinesq modeling of a rip current system, J.



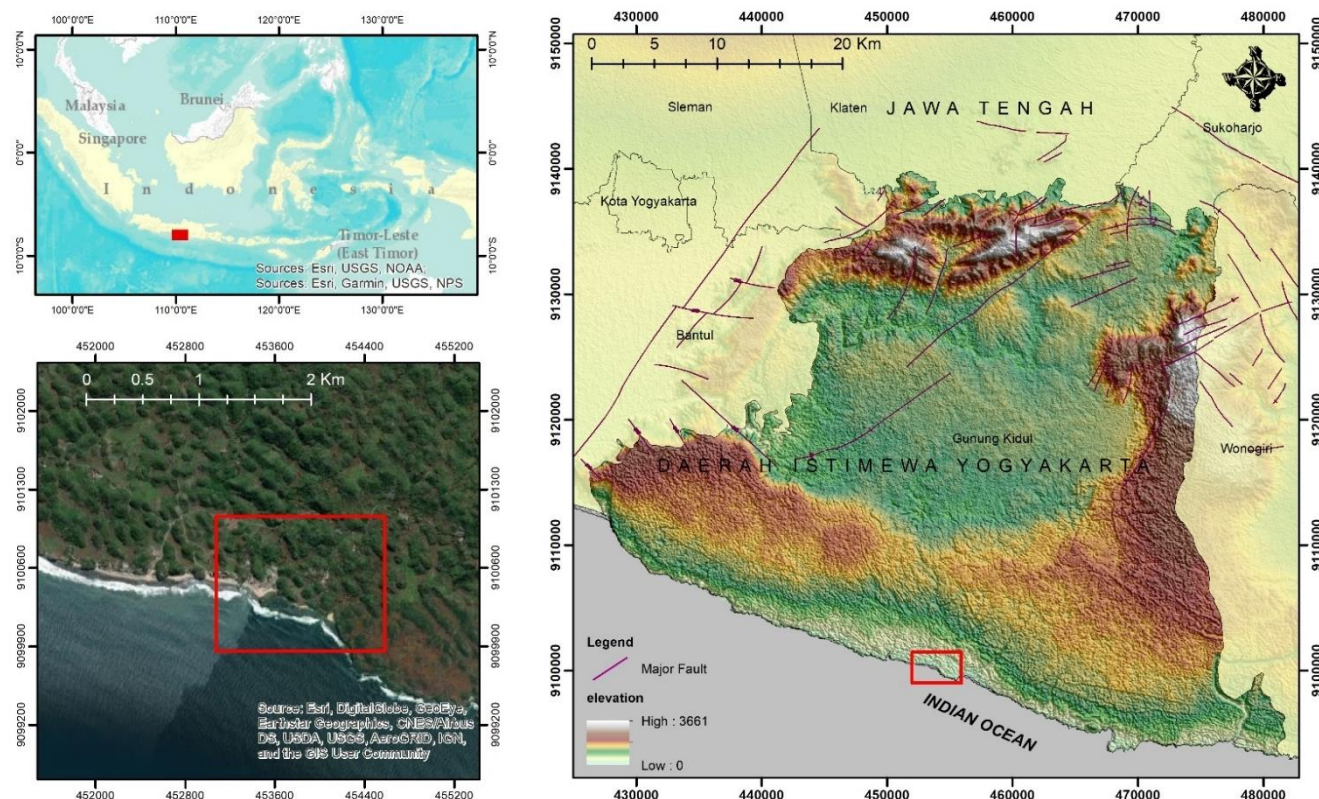
- Geophys. Res. Ocean., 104(C9), 20617–20637, doi:10.1029/1999jc900154, 1999.
- Clark, A.: Small unmanned aerial systems comparative analysis for the application to coastal erosion monitoring, *GeoResJ*, 13, 175–185, doi:10.1016/j.grj.2017.05.001, 2017.
- Disini, U.: Update Disini (@updatedisini) • Instagram photos and videos, [online] Available from:
 320 <https://www.instagram.com/p/CDBYOPhII0U/> (Accessed 23 June 2021), 2020.
- Dudkowska, A., Boruń, A., Malicki, J., Schönhofer, J. and Gic-Grusza, G.: Rip currents in the non-tidal surf zone with sandbars: numerical analysis versus field measurements, *Oceanologia*, 1–18, doi:10.1016/j.oceano.2020.02.001, 2020.
- Fallon, K. M., Lai, Q. and Leatherman, S. P.: Beachgoer’s recognition of rip current hazard at Miami Beach, Florida, *Ocean Coast. Manag.*, 165(February 2017), 63–70, doi:10.1016/j.ocecoaman.2018.08.011, 2018.
- 325 Ford, D. and Williams, P.: *Karst Hydrogeology and Geomorphology*, 2007.
- Gallop, S. L., Woodward, E., Brander, R. W. and Pitman, S. J.: Perceptions of rip current myths from the central south coast of England, *Ocean Coast. Manag.*, 119, 14–20, doi:10.1016/j.ocecoaman.2015.09.010, 2016.
- Gallop, S. L., Bryan, K. R., Pitman, S. J., Ranasinghe, R., Sandwell, D. R. and Harrison, S. R.: Rip current circulation and surf zone retention on a double barred beach, *Mar. Geol.*, 405(June), 12–22, doi:10.1016/j.margeo.2018.07.015, 2018.
- 330 Gensini, V. A. and Ashley, W. S.: Reply to “Rip Current Misunderstandings,” *Nat. Hazards*, 55(2), 163–165, doi:10.1007/s11069-010-9528-3, 2010.
- Goldscheider, N. and Drew, D.: *Methods in Karst Hydrology*, edited by N. Goldscheider and D. Drew, London., 2007.
- Gomez, C. and Purdie, H.: UAV- based Photogrammetry and Geocomputing for Hazards and Disaster Risk Monitoring – A Review, *Geoenvironmental Disasters*, 3, 23, doi:https://doi.org/10.1186/s40677-016-0060-y, 2016.
- 335 Haryono, E. and Day, M.: LANDFORM DIFFERENTIATION WITHIN THE GUNUNG KIDUL KEGELKARST , JAVA , INDONESIA, *J. Cave Karst Stud.*, 66(2), 62–69, 2004.
- Kandar: Rip Current Menjadi Faktor Utama Kecelakaan Laut Di Pantai Selatan - KH, [online] Available from: <https://kabarhandayani.com/rip-current-menjadi-faktor-utama-kecelakaan-laut-di-pantai-selatan/> (Accessed 23 June 2021), 2020.
- 340 Kasvi, E., Salmela, J., Lotsari, E., Kumpula, T. and Lane, S. N.: Comparison of remote sensing based approaches for mapping bathymetry of shallow, clear water rivers, *Geomorphology*, 333, 180–197, doi:10.1016/j.geomorph.2019.02.017, 2019.
- Kennedy, A. B. and Thomas, D.: Drifter measurements in a laboratory rip current, *J. Geophys. Res. C Ocean.*, 109(8), 1–16, doi:10.1029/2003JC001927, 2004.
- Kennedy, A. B., Zhang, Y. and Haas, K. A.: Rip Currents with Varying Gap Widths, *J. Waterw. Port, Coastal, Ocean Eng.*,
 345 134(1), 61–65, doi:10.1061/(asce)0733-950x(2008)134:1(61), 2008.
- Kršák, B., Blišťan, P., Paulíková, A., Puškárová, P., Kovanič, L., Palková, J. and Zelizňáková, V.: Use of low-cost UAV photogrammetry to analyze the accuracy of a digital elevation model in a case study, *Meas. J. Int. Meas. Confed.*, 91, 276–287, doi:10.1016/j.measurement.2016.05.028, 2016.
- Kumar, S. V. V. A., Sivaiah, B., Venkateswarlu, C., Gireesh, B., Sridevi, T., Venkateswara Rao, K., Prasad, K. V. S. R. and



- 350 Sharma, R.: Investigation of rip current processes along Visakhapatnam beaches, east coast of India: A study based on GNSS drifters and dye experiments, *J. Earth Syst. Sci.*, 130(2), doi:10.1007/s12040-021-01579-1, 2021.
- Kusumayudha, S. B., Zen, M., Notosiswoyo, S. and Gautama, R. S.: Fractal analysis of the Oyo River , cave systems , and topography of the Gunungsewu karst area , central Java , Indonesia, *Hydrogeol. J.*, 8, 271±278, 2000.
- Leatherman, S. B.: Rip Current Measurements at Three South Florida Beaches, *J. Coast. Res.*, 335, 1228–1234, doi:10.2112/jcoastres-d-16-00124.1, 2017.
- 355 Leatherman, S. P.: Rip Current: Science and Threat Communication, *J. Coast. Res.*, 72(June), 93–95, doi:10.2112/si72-017.1, 2014.
- Leon, M. P. De, Nishi, R., Kumasaka, F., Takaesu, T., Kitamura, R. and Otani, A.: Reef Rip Current Generated by Tide and Wave during Summer Season : Field Observation Conducted in Yoshiwara Coast , Ishigakijima , Okinawa , Japan , , (15), 7–
- 360 11, 2008.
- Li, Z.: Rip current hazards in South China headland beaches, *Ocean Coast. Manag.*, 121, 23–32, doi:10.1016/j.ocecoaman.2015.12.005, 2016.
- MacMahan, J. H., Thornton, E. B., Stanton, T. P. and Reniers, A. J. H. M.: RIPEX: Observations of a rip current system, *Mar. Geol.*, 218(1–4), 113–134, doi:10.1016/j.margeo.2005.03.019, 2005.
- 365 MacMahan, J. H., Thornton, E. B. and Reniers, A. J. H. M.: Rip current review, *Coast. Eng.*, 53(2–3), 191–208, doi:10.1016/j.coastaleng.2005.10.009, 2006.
- Marfai, M. A., King, L., Singh, L. P., Mardiatno, D., Sartohadi, J., Hadmoko, D. S. and Dewi, A.: Natural hazards in Central Java Province, Indonesia: An overview, *Environ. Geol.*, 56(2), 335–351, doi:10.1007/s00254-007-1169-9, 2008.
- Marfai, M. A., Sunarto, S., Khakim, N., Cahyadi, A., Rosaji, F. S., Fatchurohman, H. and Wibowo, Y. A.: Topographic data acquisition in tsunami-prone coastal area using Unmanned Aerial Vehicle (UAV), *IOP Conf. Ser. Earth Environ. Sci.*, 148(1), 0–7, doi:10.1088/1755-1315/148/1/012004, 2018.
- 370 Marfai, M. A., Fatchurohman, H. and Cahyadi, A.: An Evaluation of Tsunami Hazard Modeling in Gunungkidul Coastal Area using UAV Photogrammetry and GIS. Case Study: Drini Coastal Area, *E3S Web Conf.*, 125, doi:10.1051/e3sconf/201912509005, 2019a.
- 375 Marfai, M. A., Sunarto, Khakim, N., Fatchurohman, H., Cahyadi, A., Wibowo, Y. A. and Rosaji, F. S. C.: Tsunami hazard mapping and loss estimation using geographic information system in Drini Beach, Gunungkidul Coastal Area, Yogyakarta, Indonesia, in *E3S Web of Conferences*, vol. 76., 2019b.
- Marfai, M. A., Fatchurohman, H. and Cahyadi, A.: *Pesisir Gunungkidul*, Gadjah Mada University Press, Yogyakarta., 2020.
- Pertana, P. R.: Ini Titik Rip Current di Perairan DIY, *Biang Kecelakaan di Laut*, [online] Available from: https://travel.detik.com/travel-news/d-5127258/ini-titik-rip-current-di-perairan-diy-biang-kecelakaan-di-laut (Accessed 23
- 380 June 2021), 2020.
- Pitman, S., Gallop, S. L., Haigh, I. D., Masselink, G. and Ranasinghe, R.: Wave breaking patterns control rip current flow regimes and surfzone retention, *Mar. Geol.*, 382, 176–190, doi:10.1016/j.margeo.2016.10.016, 2016.

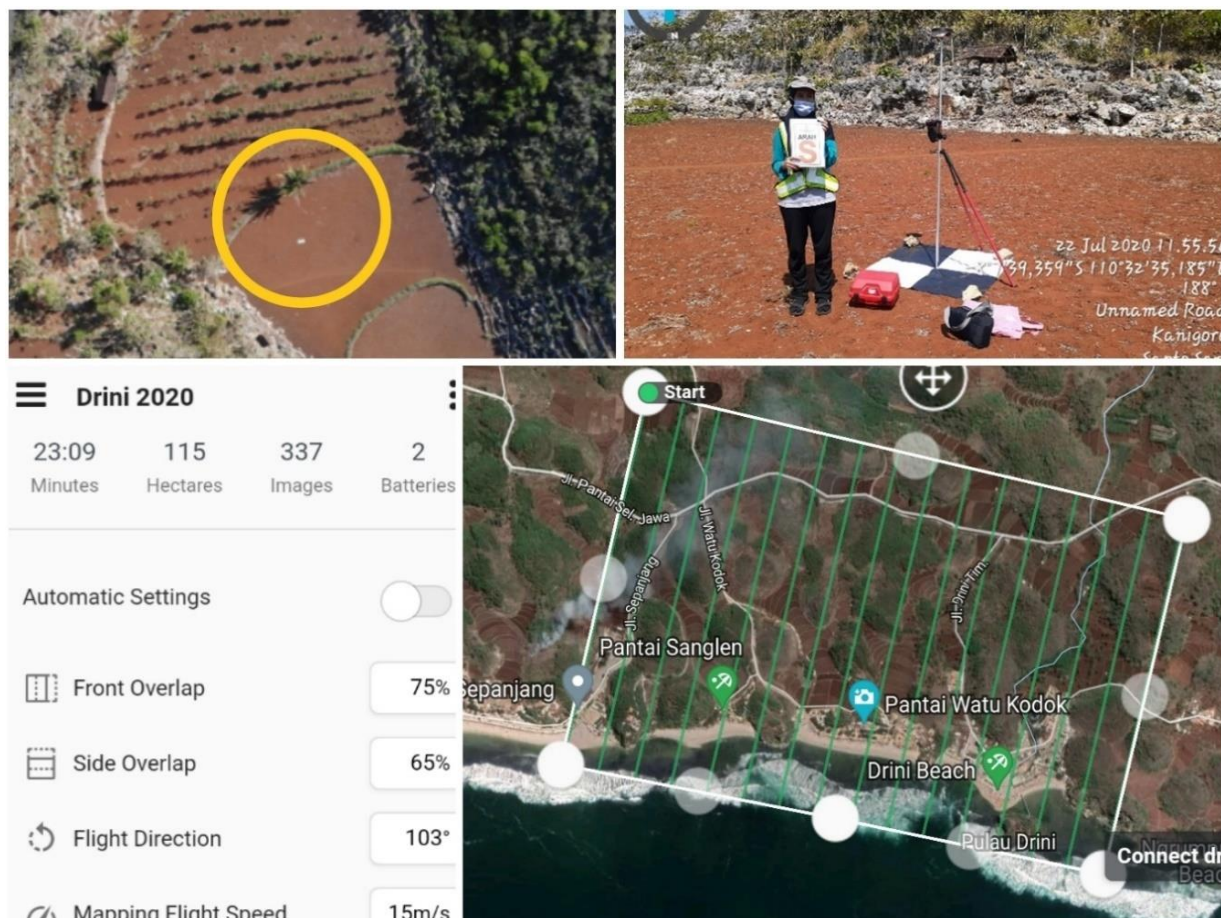


- Retnowati, A., Marfai, M. A. and Sri Sumantyo, J.: Rip Currents Signatures Zone Detection on Alos Palsar Image At
 385 Parangtritis Beach, Indonesia, Indones. J. Geogr., 44(1), doi:10.22146/indo.j.geog,2387, 2013.
- Sabet, B. S. and Barani, G. A.: Field investigation of rip currents along the southern coast of the Caspian sea, Sci. Iran., 18(4
 A), 878–884, doi:10.1016/j.scient.2011.07.017, 2011.
- Scott, T., Russell, P., Masselink, G. and Wooler, A.: Rip current variability and hazard along a macro-tidal coast, J. Coast.
 Res., 2009(SPEC. ISSUE 56), 895–899, doi:10.2307/25737708, 2009.
- 390 Scott, T. M., Russell, P., Masselink, G., Austin, M. J., Wills, S. and Wooler, A.: Rip Current Hazards on the United Kingdom,
 Rip Curr. Beach safety, Phys. Oceanogr. wave Model., (1999), 225–244, 2011.
- Da Silva, J. C. B.: SAR observation of rip currents off the Portuguese coast, Remote Sens. Eur. Seas, 399–410,
 doi:10.1007/978-1-4020-6772-3_30, 2008.
- Thi, V., Nguyet, M. and Goldscheider, N.: A simplified methodology for mapping groundwater vulnerability and
 395 contamination risk, and its first application in a tropical karst area, Vietnam, , 1666–1675, doi:10.1007/s10040-006-0069-5,
 2006.
- Turner, I. L., Harley, M. D. and Drummond, C. D.: UAVs for coastal surveying, Coast. Eng., 114, 19–24,
 doi:10.1016/j.coastaleng.2016.03.011, 2016.
- Wang, H., Zhu, S., Li, X., Zhang, W. and Nie, Y.: Numerical simulations of rip currents off arc-shaped coastlines, Acta
 400 Oceanol. Sin., 37(3), 21–30, doi:10.1007/s13131-018-1197-1, 2018.
- Widartono, B. S., Wachid, M. N., Umarhadi, D. A., Azizah, A. N. and Cahyo, R. D.: Kite Aerial Photography (KAP) for rip
 current identification in Parangtritis Beach, E3S Web Conf., 76, 1–5, doi:10.1051/e3sconf/20197603005, 2019.
- Widiyanto, D.: Kecelakaan Laut 2019 Terjadi 90 Kasus, 15 Orang Meninggal, [online] Available from:
 https://www.krjogja.com/berita-lokal/diy/gunungkidul/kecelakaan-laut-2019-terjadi-90-kasus-15-orang-meninggal/
 405 (Accessed 15 June 2021), 2020.
- Winter, G., Van Dongeren, A. R., De Schipper, M. A. and Van Thiel de Vries, J. S. M.: Rip currents under obliquely incident
 wind waves and tidal longshore currents, Coast. Eng., 89, 106–119, doi:10.1016/j.coastaleng.2014.04.001, 2014.
- Yuwono, M.: Rip Current, Penyebab Banyaknya Wisatawan Terseret Arus Pantai Selatan Gunungkidul, [online] Available
 from: https://regional.kompas.com/read/2020/07/24/16312461/rip-current-penyebab-banyaknya-wisatawan-terseret-arus-
 410 pantai-selatan (Accessed 23 June 2021), 2020.



415

Figure 1: The Study area location (up left (© Esri, NOAA, USGS, Garmin 2021)).The Drini Beach surrounded by conical karst landforms (bottom left (© Google Earth 2021)) and the northwest-southeast fault with a northeastern synclinal axis in the middle (right)



420 **Figure 2: An example of Ground Control Point measurement using the Real-Time Kinematic method. The visual appearance of a marker from the aerial photo (top left) and field photo reference (top right). The flight mission and path settings at Drini Beach were determined in the application DroneDeploy (© Google Earth 2021).**

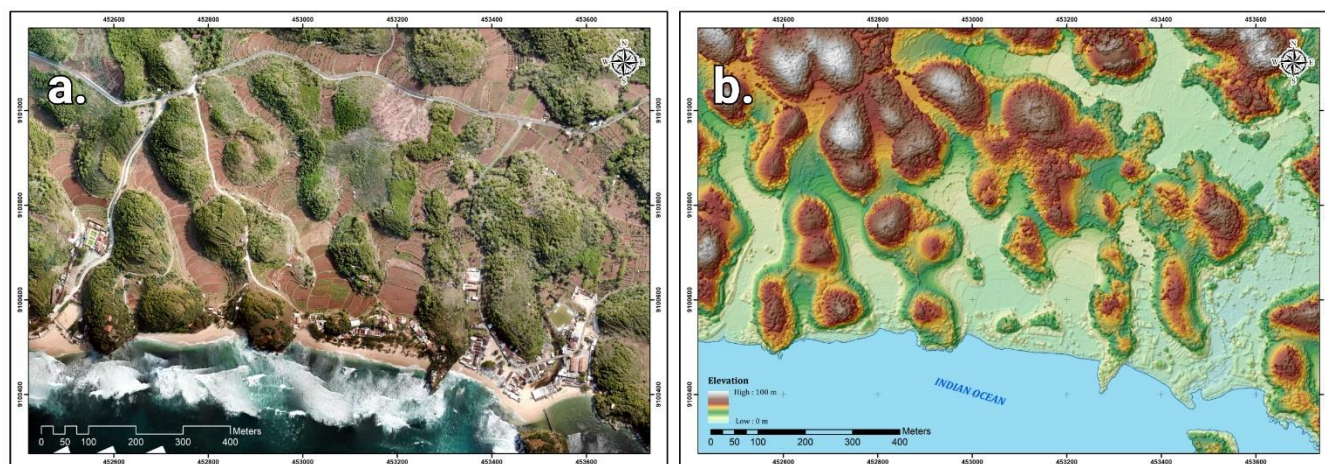


Figure 3: The orthophoto results with 7 cm Ground Sample Distance (a) and Digital Surface Model with approximately 35 cm spatial resolution

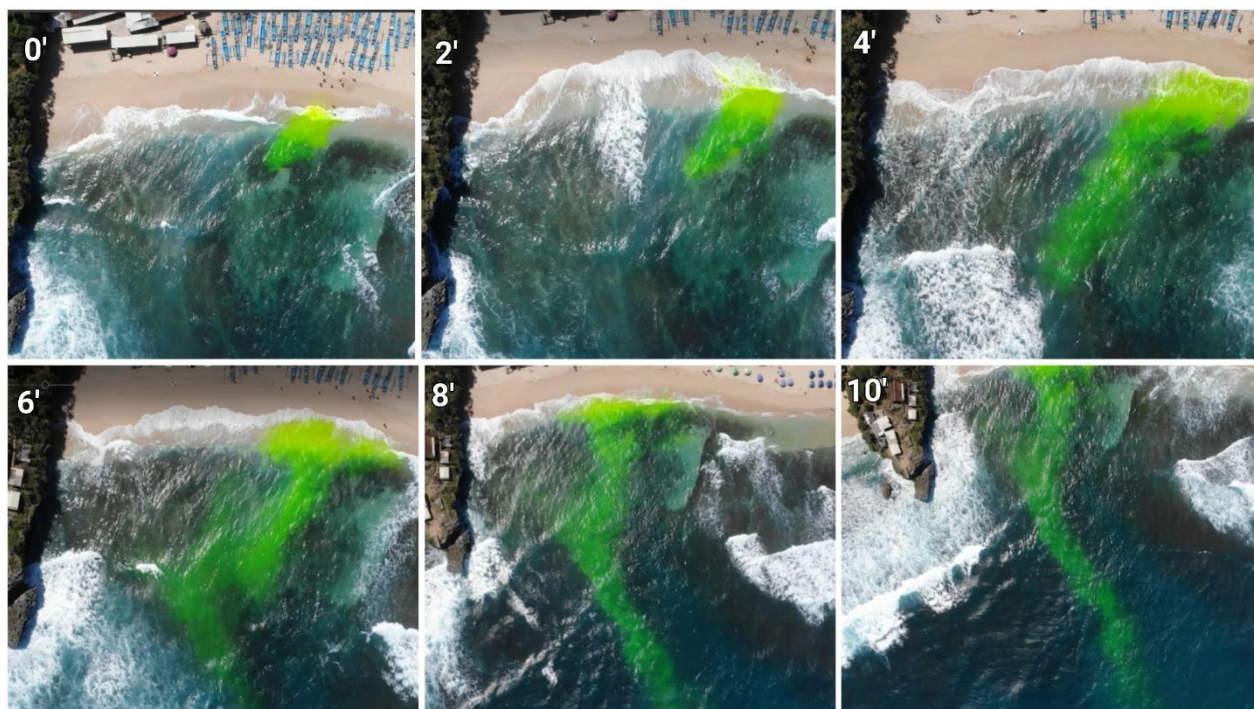


Figure 4 : Video clips showing the movement of the fluorescent dye during the rip current tracing. The development stage starts with feeder currents in Minutes 0 to 2, which then entered the neck in Minutes 4–8 and reached the head in Minutes 10.

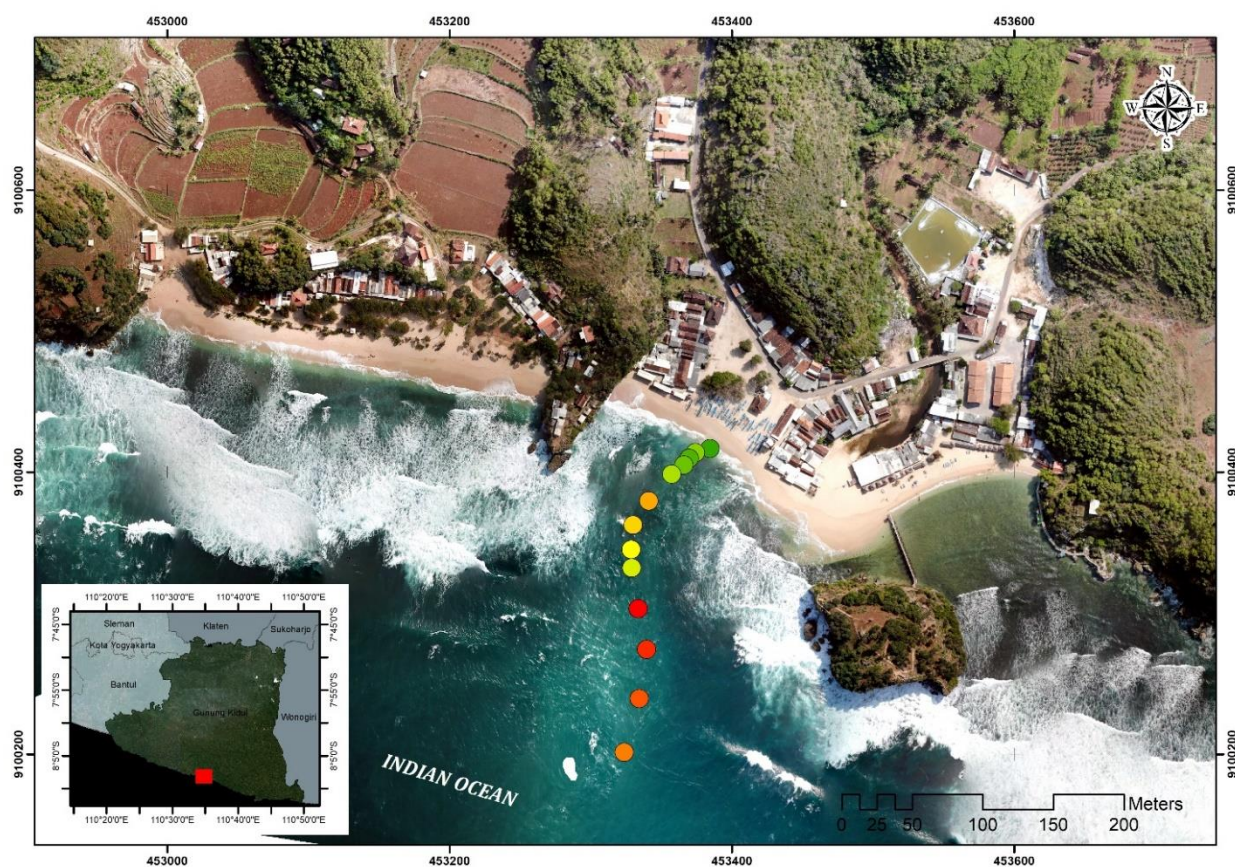


Figure 5: Orthomosaic image overlaid with the direction and velocity of the tracer dye movement, as estimated from the video sequence. The color gradation, from green to red, indicates different speeds of the rip current.



435 **Figure 6: Temporal observation of Google Earth imagery from 2007 to 2019 shows a persistent gap in the surf zone. The images also indicate a rapid change in land use to support the increasing tourism activities (© Google Earth 2021) .**



440 **Figure 7: Aerial views of the rip current location at the peak low tide on October 20, 2019, at 06:55 am, where the reef flat was not submerged (a), and moments before the low tide on July 22, 2019, at 09:25 am, where the rip current is the most dangerous (b)**



Figure 8: The gap in the reef flat moments before the low tide. The photo taken on July 25, 2020, at 12:15 am (a) shows no tourists were on the beach due to restrictions on tourism activities imposed to curb the spread of the COVID-19 pandemic. The photo taken on May 16, 2021, at 04:22 pm (b) shows beach visitors playing in the gap during low tide. This gap is safe for swimmers at peak low tide because of insufficient feeder currents.



Table 1 Tracer dye movement's speeds per minute

Minute	Distance (m)	Speed (m/s)
0	0.00	0.00
1	10.62	0.18
2	5.90	0.10
3	6.04	0.10
4	10.77	0.18
5	24.90	0.42
6	20.40	0.34
7	17.50	0.29
8	12.80	0.21
9	39.57	0.66
10	35.30	0.59
11	29.50	0.49
12	29.20	0.49